

# Polysulphone and poly(phenylene sulphide) blends: 1. Thermal characterization and phase morphology

M.-F. Cheung, A. Golovoy, H. K. Plummer and H. van Oene

Research Staff, Ford Motor Company, PO Box 2053, Dearborn, MI 48121, USA

(Received 16 August 1989; accepted 20 October 1989)

The phase behaviour and morphology of injection moulded specimens of polysulphone (PSF) and poly(phenylene sulphide) (PPS) blends were studied by differential scanning calorimetry (d.s.c.), dynamical mechanical thermal analysis (d.m.t.a.) and transmission electron microscopy (TEM). The blends are phase separated regardless of the blend composition as revealed by d.s.c., d.m.t.a. and TEM. Upon annealing at 160°C for 2 h, d.m.t.a. results indicate that the PPS phase remains in the amorphous state at compositions <10%. At compositions between 20 and 35%, the PPS appears to be dispersed in a mixed mode of amorphous and crystalline domains. Above 35% the PPS phase appears to become fully crystallized upon annealing of the blends. At 10% PPS, TEM results showed 35–200 nm size dispersion both in the as-moulded and in the annealed specimens. At 20% the PPS phase varied widely in size, from 35 nm to tens of micrometres but remained as an included phase. TEM also revealed a compound morphology of the included phase at a composition of 50 wt% of each component.

(Keywords: blends; polysulphone; poly(phenylene sulphide); thermal properties; morphology)

## INTRODUCTION

Polysulphone (PSF) is one of the useful high performance engineering thermoplastics with outstanding thermal and mechanical properties. Its high resistance to hydrolysis at elevated temperature is known<sup>1</sup>. However, this amorphous polymer exhibits poor organic solvent resistance. Moreover, it requires a high processing temperature due to its high glass transition temperature. Poly(phenylene sulphide) (PPS), on the other hand, is a semicrystalline high performance plastic with outstanding chemical resistance. It has excellent short and long term heat resistance, and is known to be low in moisture absorption, too. It has excellent and balanced mechanical properties except that, when fully crystallized, it tends to become brittle. Other properties are also affected by crystallinity<sup>2</sup>.

When PPS is blended with PSF, especially under melt-extrusion conditions, the blending may bring some benefits into the system such as chemical resistance, ease of processing and moisture resistance, which is inherited from both ingredients. Since both PSF and PPS are aromatic and contain sulphur, one may also expect some degree of chemical interaction between the two systems.

PSF or PPS blends with other polymers have been reported in the literature<sup>3–7</sup>. Almost all investigations, however, were done on materials prepared by solution mixing. Zeng and Mai<sup>3</sup> investigated PSF/PPS blends using solution mixing and reported that phase separated blends were obtained after solvent evaporation. They concluded that a heat treatment, to above 300°C, is important to gain better properties for the PPS resin. Zeng and co-workers<sup>4</sup> discussed the crystalline morphologies of poly(phenylene sulphide) and its blends with polysulphone.

In this paper, we report the thermal behaviour and the phase morphology of the PSF/PPS blends prepared by

conventional melt-extrusion and injection moulding. The thermal behaviour of the blends as-moulded and annealed at 160 or 190°C for 2 h are discussed. Differential scanning calorimetry (d.s.c.), dynamic mechanical thermal analysis (d.m.t.a.) and heat deflection temperature (h.d.t.) were used for thermal characterization. Transmission electron microscopy (TEM) was used to study morphology. In a second paper we will report the mechanical properties of these blends.

## EXPERIMENTAL

### Raw materials

Polysulphone (Udel-1700) was obtained from Amoco Performance Products Inc. Poly(phenylene sulphide), Fortron 214P, was supplied by Celanese Engineering Resins Inc. Materials were vacuum dried at 110°C for at least 16 h before extrusion.

### Melt extrusion

A Haake Rheomex 254 single screw extruder was used to extrude the blends. The temperature was set at 285–300°C at different zones of the extruder. The residence time of the melted materials in the extruder was estimated to be  $\approx$  2 min. Compositions of the blends prepared were 10, 20, 30, 35, 45, 50 and 70 wt% PPS.

### Injection moulding

A BOY 50M injection moulding machine was used for moulding test specimens with an ASTM standard specimen mould. Blend extrudates were pre-dried at 110°C in a forced air oven for at least 16 h before injection moulding. The mould temperature was set at 60°C throughout all moulding experiments except for the pure

PPS moulding, where the mould temperature was set at 21°C. The temperature along the barrel was set at 290–327°C for all blend compositions. Only the injection pressure was changed at different compositions. In general, the higher the PPS content, the lower the injection pressure required. Tensile bars of PPS, 0.3175 cm thick after injection moulding, show opaqueness as an indication of crystallinity. Flash from the side of the bars gave an amber clear film, 0.75 mm thick, which was used to provide samples of amorphous PPS for d.m.t.a. scans.

## THERMAL CHARACTERIZATION

### Differential scanning calorimetry

D.s.c. experiments were done in a Mettler DSC-30 calorimeter. The Mettler TC10A control and evaluation module was used to collect data and evaluate the results. Thermograms were traced from 30 to 300°C with a scanning rate of 5°C min<sup>-1</sup> for all analyses. During repetitive scanning, at the end of each scan, the control module needed about 5 min to evaluate and transmit the data to the computer. Until the entire evaluation and data transmission process was finished the calorimeter was held at the maximum temperature and thereafter returned to the starting temperature.

### Dynamic mechanical thermal analysis

A PL-DMTA from Polymer Laboratories was used. Tests were obtained from -100 to 250°C using a scanning rate of 1°C min<sup>-1</sup> at oscillating frequencies of 0.1, 1.0 and 10 Hz. Data collection and evaluation used software supplied by Polymer Laboratories. Samples were run using the dual cantilever bending mode. Sample geometry was designed so that the sample geometry constant  $-\log_{10} k$  was  $\leq 4$  as calculated by the computer software from the sample dimensions.

### Heat deflection temperature measurement

Heat deflection temperatures were measured using an ASTM method (D648) with a Tinius Olsen instrument at a load of 1.8 MPa.

### Transmission electron microscopy

Interior portions of each blend test bar were removed and oriented such that the plane of observation, of sections microtomed from the bar, was perpendicular to the mould flow direction. Microtomed thin sections for TEM observation were obtained from as-moulded blends containing 10, 20, 35, 50 and 70% PPS in PSF using an LKB Ultratome III with a Diatone diamond knife. Microtomed thin sections of the blends after annealing at 160°C for 2 h were also similarly prepared for TEM. The thin (50 nm) sections of the as-moulded and annealed blends, supported on carbon film substrates on TEM grids were examined by bright field TEM (BF TEM) in a Siemens 102 TEM operated at 100 keV. Due to sufficient electron contrast difference between the PPS phase (dark) and the PSF phase (light) no etching or staining techniques were used in this study.

## RESULTS AND DISCUSSION

The d.s.c. thermograms of injection moulded PSF and PPS are shown in *Figure 1*. The sample used for PPS (curve a) was a portion of the clear amber mould flash

from injection moulding. It represents the amorphous state of the sample with a glass transition temperature ( $T_g$ ) at 88°C and a cold crystallization temperature ( $T_c$ ) at  $\approx 120^\circ\text{C}$ . The melting temperature ( $T_m$ ) was recorded as 285°C on the initial scan. The  $T_g$  of the PSF (curve c) was found to be at 185°C on the initial scan. When the sample of PPS was cooled from 300 to 30°C ( $\approx 3$  min) and rescanned using the same heating program, no cold crystallization exotherm was found and the  $T_g$  shifted to higher temperature ( $\approx 100$  or slightly higher, although it is difficult to detect the transition from the present thermogram). This phenomenon has been reported recently<sup>8</sup>. This result indicates that the rate of crystallization of PPS is relatively fast even with such a rapid cooling rate and the sample appears to be in the crystalline state under the present cooling condition. *Table 1* lists the results of four consecutive scans of the same samples of PSF and PPS. For PSF, after four consecutive scans, there appears to be no appreciable change of  $T_g$ . The melting temperature of the PPS did change after the first scan but remained constant thereafter. As one would expect, the melting temperature could be affected by the perfection of the crystal structure. The data indicate that both PSF and PPS are thermally stable in the scanning temperature range from 30 to 300°C.

A d.s.c. thermogram for a blend of 80% PSF and 20% PPS is shown in *Figure 2*. The first scan of an injection moulded sample shows the  $T_g$  of amorphous PPS, a cold

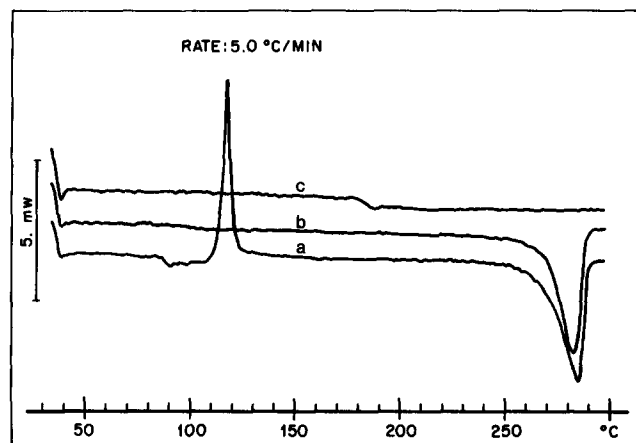


**Figure 1** D.s.c. thermograms of: (a) PPS amorphous; (b) PPS second scan; (c) PSF

**Table 1** D.s.c. results of multiple scans

	Run	$T_g$ (°C)	$T_c$ (°C)	$T_m$ (°C)	$\Delta H_f$ (J g <sup>-1</sup> )
PPS	1	87.3	119	285	42.0
	2	—	—	281.5	41.1
	3	—	—	282.0	39.6
	4	—	—	282.0	39.7
PSF	1	183.8	—	—	—
	2	184.2	—	—	—
	3	184.8	—	—	—
	4	185.0	—	—	—

$T_g$ , glass transition temperature  
 $T_c$ , cold crystallization temperature  
 $T_m$ , melting temperature  
 $H_f$ , heat of fusion

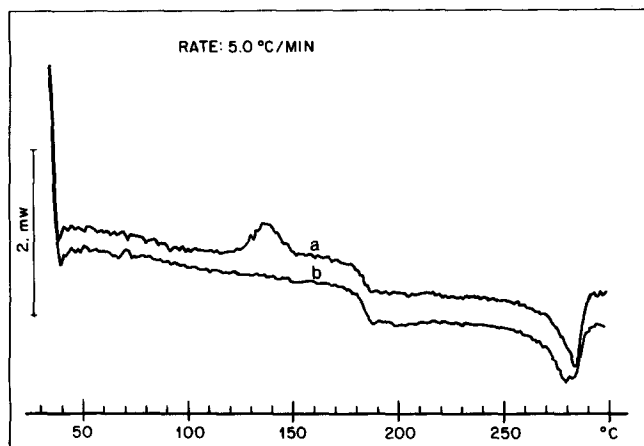


**Figure 2** D.s.c. thermograms of PSF/PPS (80/20 by weight) blend: (a) as moulded, mould temperature set at 60°C; (b) annealed 190°C for 2 h

**Table 2** D.s.c. results of blends annealed at 190°C for 2 h<sup>a</sup>

PPS (%)	$T_g$ (°C) <sup>b</sup>	$T_m$ (°C)	$\Delta H_f$ (J g <sup>-1</sup> )	$\Delta H_f$ (J g <sup>-1</sup> ) <sup>c</sup>
0	184.7	—	—	—
10	183.1	—	0–1.5	4.2
20	183.6	282.7	5.9 (29.0%) <sup>d</sup>	8.3
30	182.7	283.5	10.4 (16.8%) <sup>d</sup>	12.5
35	182.8	283.9	13.4 (8.2%) <sup>d</sup>	14.6
45	181.9	284.8	18.3 (2.1%) <sup>d</sup>	18.7
50	181.7	284.0	19.7 (5.3%) <sup>d</sup>	20.8
70	180.7	284.4	28.2 (3.1%) <sup>d</sup>	29.1
100	—	284.7	41.6	—

<sup>a</sup> Average value of nine specimens

<sup>b</sup> Transition temperature of PSF phase

<sup>c</sup> Calculated value: 41.6 J g<sup>-1</sup> as 100 wt%

<sup>d</sup> Amorphous fraction

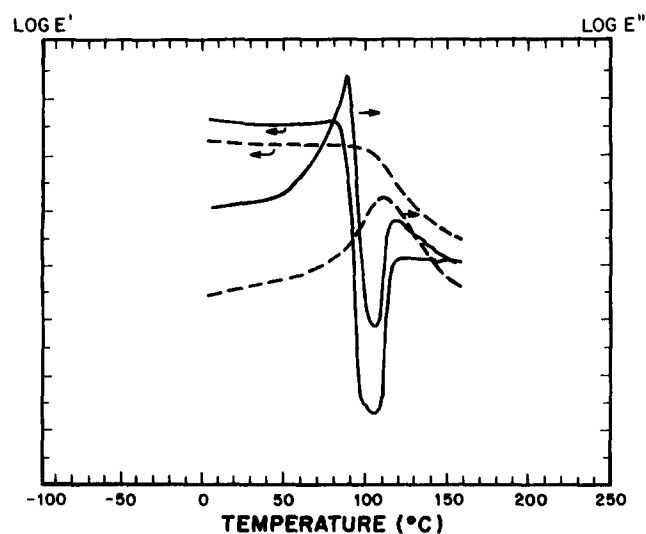
crystallization peak, the  $T_g$  of PSF and a melting peak of PPS. After annealing for 2 h at 190°C, the  $T_g$  of PPS and the cold crystallization peak have disappeared. Only the  $T_g$  of PSF and a melting peak of PPS are evident.

Table 2 lists the transition temperatures from d.s.c. experiments of all the blends after annealing at 190°C for 2 h. The annealing temperature of 190°C was chosen to avoid confusion with the annealing endotherm and the  $T_g$  of PSF, which may coexist in the same temperature region. The  $T_g$  of the PSF phase decreases somewhat, the peak melting temperature of the PPS phase increases. From the observed melting peak, an amorphous fraction can be calculated, which is also listed in Table 2. Blends with 10, 20, 30 and 35 wt% PPS contain a significant amorphous fraction. Blends with larger amounts of PPS seem to be as fully crystallized as and have a similar melting temperature to PPS itself. The d.s.c. data show that, upon annealing, the glass transition of amorphous PPS is not discernible, and only a melting peak remains to signify the presence of PPS.

To characterize the blends further, the dynamic mechanical properties were determined. In Figure 3 a d.m.t.a. scan of injection moulded PPS is shown. The amorphous sample was taken from the mould flash, which was amber and transparent. The storage modulus  $E'$  shows a sharp decrease around 80°C, followed by an increase, which levels off at  $\approx 120^\circ\text{C}$ . From the d.s.c. data it is clear that this behaviour is due to the crystallization

of PPS. Also shown are the data for an annealed PPS sample. From the d.s.c. analysis we know that no further crystallization occurs. No  $T_g$ -type transition is apparent in the storage modulus  $E'$  around 90°C. Instead one observes a transition associated with a loss process that is centred around 109°C. One may attribute this transition to the glass transition of the amorphous phase of crystallized PPS. The increase in  $T_g$  with crystallization is common to many semicrystalline polymers and has been reviewed recently by Struik<sup>9</sup>.

Similar dynamic mechanical data were obtained for a blend of 80% PSF and 20% PPS as shown in Figure 4. The injection moulded sample again shows  $E'$  to decrease sharply at 80°C, levelling off at 100°C and increasing at 120°C. The loss modulus,  $E''$ , shows a broad feature, which is difficult to interpret precisely. The annealed sample, however, shows at least three distinct loss processes ( $E''$ ), a process associated with wholly amorphous PPS at  $\approx 85^\circ\text{C}$ , a broad feature associated with the amorphous phase in crystallized PPS centred around 110°C and the glass transition of PSF at 180°C. Hence, on annealing some of the PPS phase does not crystallize.



**Figure 3** D.m.t.a. thermogram at 0.1 Hz of PPS: —, amorphous; ----, annealed at 160°C for 2 h (curves shifted along the ordinate)

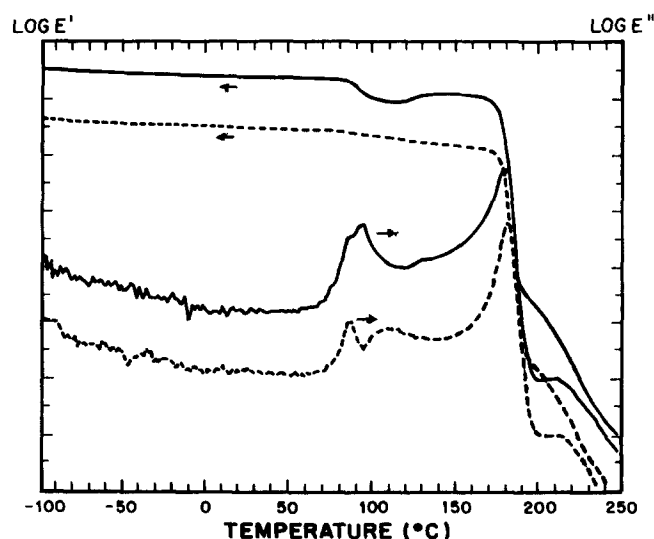


**Figure 4** D.m.t.a. thermogram at 0.1 Hz of PSF/PPS blend (80/20 by weight): —, as moulded; ----, annealed at 160°C for 2 h

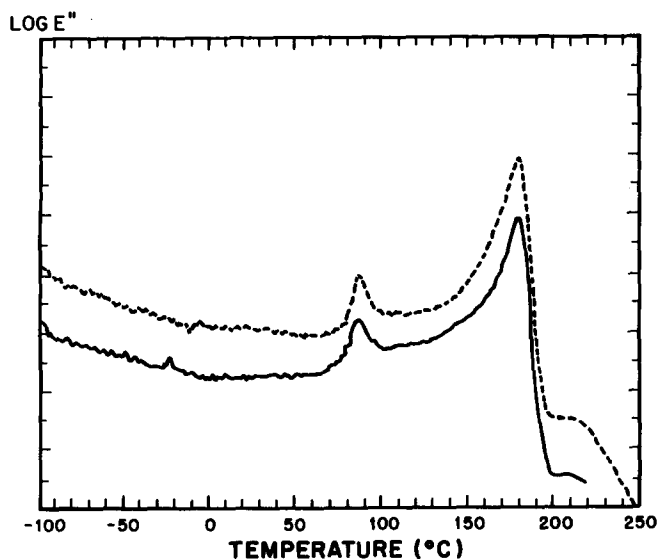


**Figure 5** D.m.t.a. thermogram at 0.1 Hz of PSF/PPS blend (90/10 by weight): —, as moulded, mould temperature set at 60°C; ----, annealed at 160°C for 2 h (curves shifted along the ordinate)

**Table 3** Loss modulus peak temperature of blends as moulded<sup>a</sup>

PPS (%)	T <sub>1</sub> (°C)	T <sub>2</sub> (°C) <sup>b</sup>	T <sub>3</sub> (°C)
0	—	—	181
10	86	—	179
20	86 (shoulder) 93	—	179
30	92	121	177
35	93	121 (weak)	177
45	93	118	177
50	93	115	177
70	89	115	177
100	87 <sup>c</sup>	—	—

<sup>a</sup> Mould temperature set at 60°C

<sup>b</sup> Cold crystallization transition

<sup>c</sup> Mould temperature set at 21°C

**Table 4** Loss modulus peak temperature of blends annealed at 160°C for 2 h

PPS (%)	T <sub>1</sub> (°C)	T <sub>2</sub> (°C) <sup>b</sup>	T <sub>3</sub> (°C)
0	—	—	181
10	87	—	179
20	85	110	178
30	87 (weak)	110	178
35	86 (weak)	107	177
45	—	109	178
50	—	108	177
70	—	108	177
100	—	109	—

This confirms the finding from d.s.c. indicating an amorphous fraction of ≈29% (Table 2).

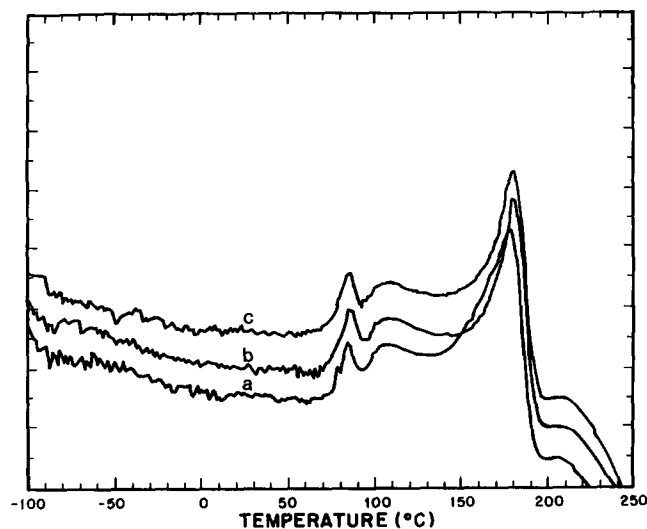
On this basis, the 10% PPS–90% PSF blend, which according to d.s.c. measurement contains essentially no crystalline PPS, should show two transitions only (*E''*), one at 86°C, due to the amorphous PPS, and one at 179°C, due to the glass transition of PSF. This is indeed what is found, as shown in Figure 5.

Table 3 lists the transition temperatures taken from the loss modulus (*E''*) of the as-moulded blend samples. The transition temperatures of the blends after annealing at 160°C for 2 h are listed in Table 4. With PPS <10%, the blend fails to crystallize even when annealed at 160°C

for 2 h. From 20 to 35% PPS, the blends exhibit three transition peaks, which correspond to the amorphous regions of both the crystallized and uncrystallized phases of PPS plus that of the PSF phase. The lower the PPS content, the more pronounced is the uncrystallized amorphous phase transition. The PSF transition remains essentially the same. Zeng and co-workers<sup>4</sup> studied the morphologies of solution blends of PSF/PPS and indicated that, at high PSF concentration, the PPS phase may not crystallize due to chain expansion and entanglement.

Figure 6 shows the d.m.t.a. results of the 20% PPS–80% PSF blend which had been subjected to different temperatures and duration of annealing. All the scans show that the existence of two transitions in the amorphous region of PPS is independent of the annealing temperature as well as the duration of the annealing. Annealing at 190°C, which is slightly above the *T<sub>g</sub>* of PSF, also showed two transition temperatures (Figure 6c).

Heat deflection temperatures (h.d.t.) of the annealed samples, at 1.8 MPa, are listed in Table 5. A plot of storage modulus (*E'*) versus temperature of the annealed samples with the h.d.t. indicated by circles on the modulus curves is shown in Figure 7. Below 50% PPS, the h.d.t. is close to the PSF glass transition temperature. This indicates that the h.d.t. is dominated by the continuous phase and only slightly influenced by the dispersed domains, which have a lower *T<sub>g</sub>*. At 50% PPS, the h.d.t. differ by about 15°C from that of PSF.



**Figure 6** D.m.t.a. thermogram at 0.1 Hz of PSF/PPS blend (80/20 by weight) annealed at: (a) at 160°C for 2 h; (b) 160°C for 16 h; (c) 190°C for 2 h (curves shifted along the ordinate)

**Table 5** Heat deflection temperature of blends at 1.8 MPa (°C)

PPS (%)	As moulded <sup>a</sup>	Annealed <sup>b</sup>
0	167	179
10	161	171
20	156	168
35	153	166
50	131	164
70	95	134
100	88 <sup>c</sup>	116

<sup>a</sup> Mould temperature set at 60°C

<sup>b</sup> Annealed at 160°C for 2 h

<sup>c</sup> Mould temperature set at 21°C

Figures 8–12 are bright field TEM micrographs showing the morphology of the as-moulded and annealed samples as viewed perpendicular to the melt flow direction. In each micrograph the double-headed arrow indicates the melt flow direction during injection moulding. The single-headed arrows show the direction in which the diamond knife travelled through the sample during microtome sectioning. Artefacts caused by debris attached to the knife edge from previous sections are seen as parallel lines which are thinner than the rest of the section. Artefacts caused by compression of the polymer blend by the knife (oval rather than spherical second-phase particles) can also be seen in many of the micrographs.

The 10% PPS–90% PSF blend (Figure 8) shows a morphology consisting of a PSF matrix and a dark PPS included phase. Some regions contain spherical PPS domains ranging in size from  $\approx 35$  to 200 nm (Figure 8a).

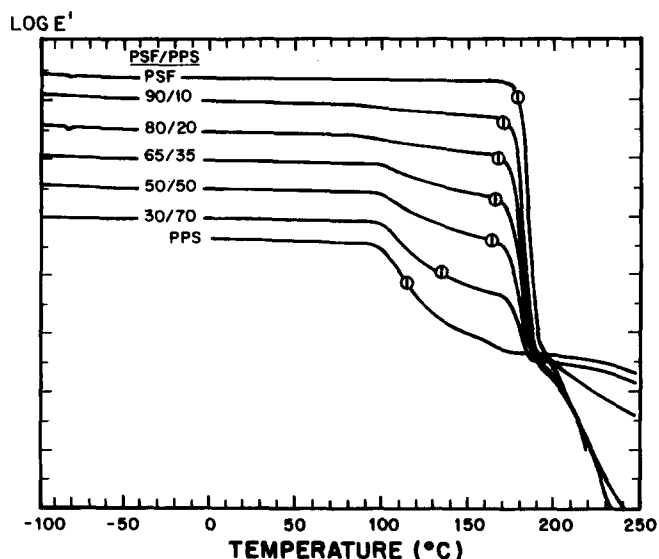


Figure 7 D.m.t.a. thermogram at 0.1 Hz of PSF/PPS blends annealed at 160°C for 2 h: plot of loss modulus versus temperature; , heat deflection temperature

Other regions contain spherical and elongated stratified sheets of the PPS phase as large as  $0.35 \mu\text{m} \times 2.5 \mu\text{m}$  (Figure 8b). The particles and stratified sheets are aligned along the mould flow direction. After annealing (Figure 8c) the spherical PPS phase increases slightly, if at all, in average size, with the largest  $\leq 0.3 \mu\text{m}$ . Most of the larger PPS inclusions were compressed to an oval shape during microtome sectioning. The slight change in the PPS dispersion size, if caused by annealing, would suggest little or no change in the PPS phase crystallinity, which is borne out by the d.m.t.a. results. That the change in the PPS size is more likely to be due to sample heterogeneity (this sample was not cut from the same sample bar as the unannealed sample, Figure 8a and b) than to annealing is evidenced by the heterogeneous morphology seen in the 20% PPS blend.

Examination of the 20% PPS blend shows the as-moulded blend, Figure 9a, to contain a PSF matrix and a spherical included PPS phase with a rather heterogeneous size distribution. The PPS inclusions in this sample vary in size from  $\approx 70$  nm spheres, to  $\approx 0.3 \mu\text{m}$  spheres, to long stratified sheet inclusions many micrometres long. The later stage of droplet formation from stratified sheets, seen in Figure 9a, is evident in Figure 9b. After annealing at 160°C for 2 h, the PPS phase shows little or no change attributable to annealing. An additional experiment was done to try to find a morphological analogue to the amorphous/crystalline phases observed by d.m.t.a. In that experiment thin microtomed sections, of the as-moulded sample, on electron microscope grids were annealed at 160°C for 2 h. The annealed cross sections showed no changes to the PPS phase attributable to this annealing procedure either. Also evident in this blend, as with the 10% blend, is a definite alignment of the PPS phase spherical inclusions along the flow direction.

At 35% PPS concentration the morphology changes from a simple included phase in a matrix to a more complex morphology. At this concentration there is evidence, shown in Figure 10a, that the PPS phase and the PSF phase could be a co-continuous matrix with

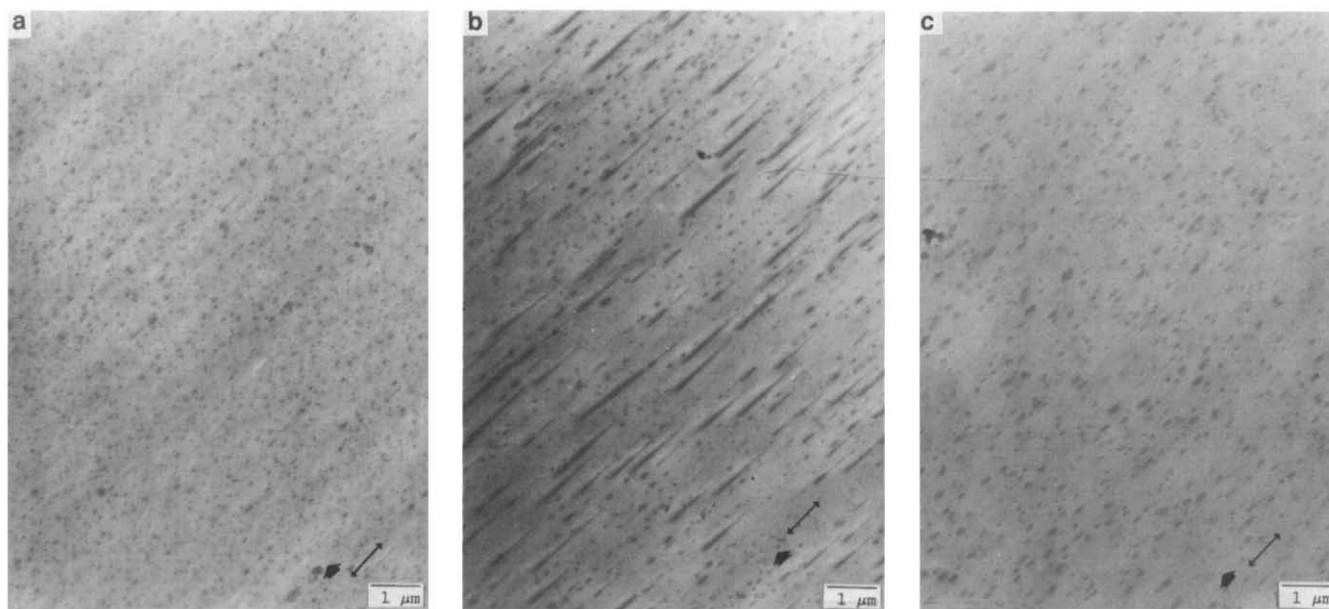


Figure 8 TEM micrograph of PSF/PPS blend (90/10 by weight): (a), (b) as moulded; (c) annealed

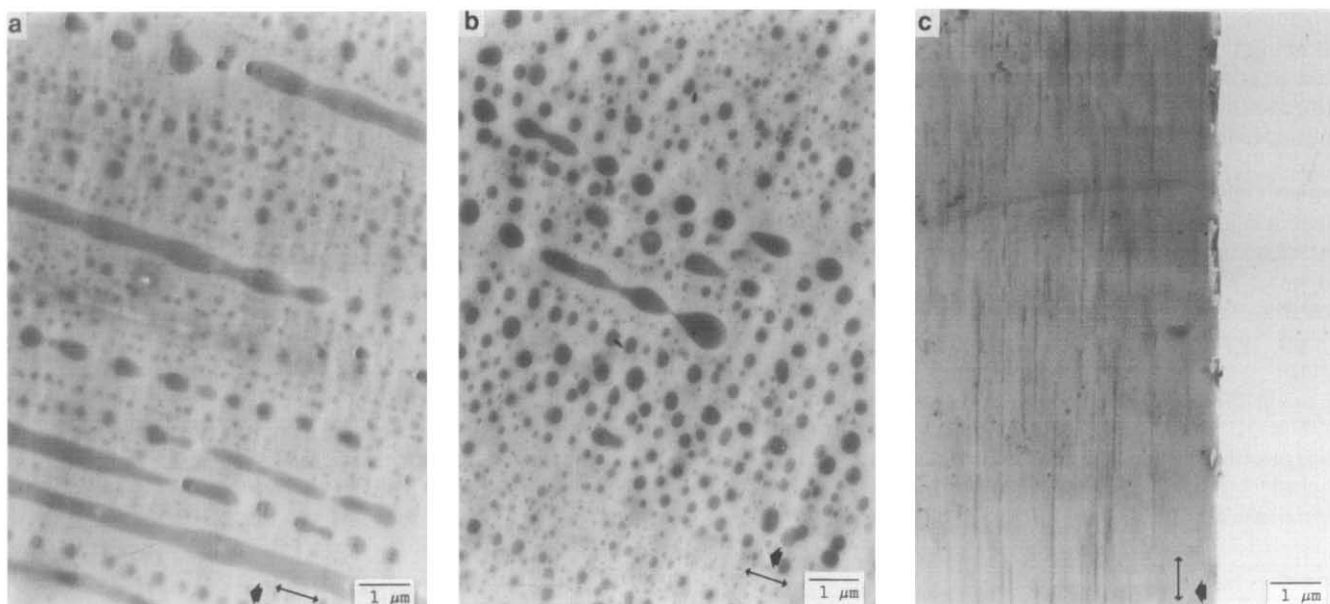


Figure 9 TEM micrograph of PSF/PPS blend (80/20 by weight): (a), (b) as moulded, bulk area; (c) as moulded, surface

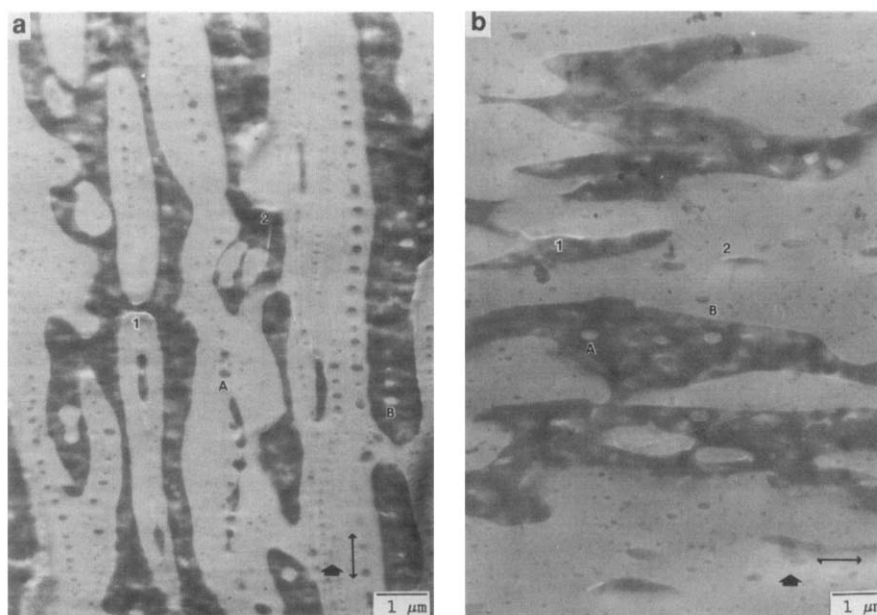


Figure 10 TEM micrograph of PSF/PPS blend (65/35 by weight): (a) as moulded; (b) annealed

some included phase. Both components are present as stratified zones, many of which are as long or longer than  $10\ \mu\text{m}$ . The layers are oriented along the flow direction. Both components are also present as included phase spheres or irregular oval shapes such as seen at points A and B in Figures 10a and b. The morphology after annealing at  $160^\circ\text{C}$  for 2 h is seen in Figure 10b. Small oval inclusions of both components of the blend remain after annealing. In this figure the oval shapes are formed by compression during microtome sectioning. Also evident in Figure 10 are boundary regions between the two phases which have been torn during microtomy (points 1 and 2).

The morphology of the as-moulded 50% PPS blend is shown in Figure 11a. The complex morphology consists of large elongated phases of each component and small

spherical inclusions of one component within the larger phases of the other component. Figure 11b shows the morphology of the 50% blend after annealing at  $160^\circ\text{C}$  for 2 h. The light phase (PSF) has a highly irregular shape when it is surrounded by PPS (the dark phase). The shape of the boundary is essentially convex with respect to the PSF phase. This blend also contains boundary interface tears, such as at points 1 in Figures 11a and b, because of microtome sectioning.

The morphology of the as-moulded 70% PPS blend is seen in Figure 12. The PPS phase, as expected, is the matrix phase with roughly spherical inclusions of PSF up to  $6\ \mu\text{m}$  diameter. Although this blend, containing a high PPS concentration, was not annealed, the morphology seen by TEM would not be expected to change from that seen in the as-moulded state.

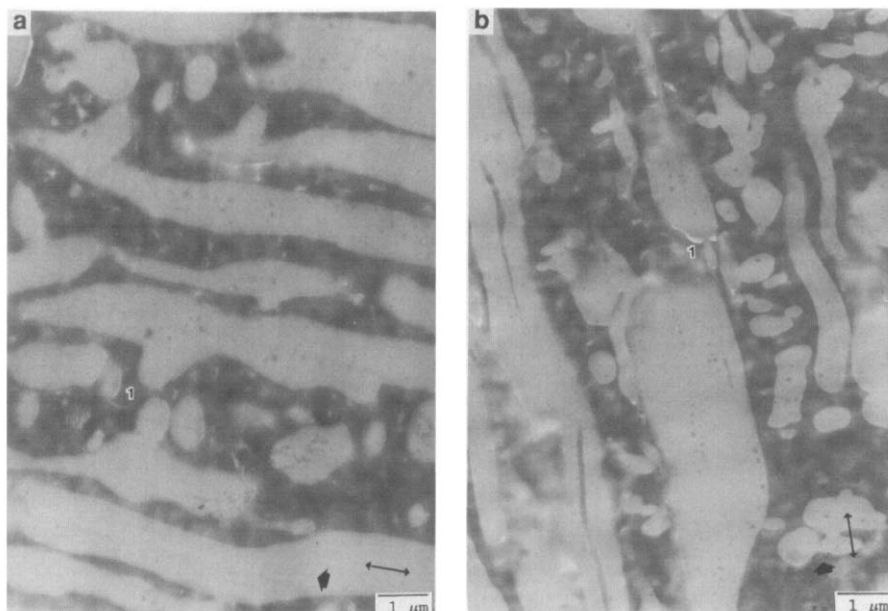


Figure 11 TEM micrograph of PSF/PPS blend (50/50 by weight): (a) as moulded; (b) annealed

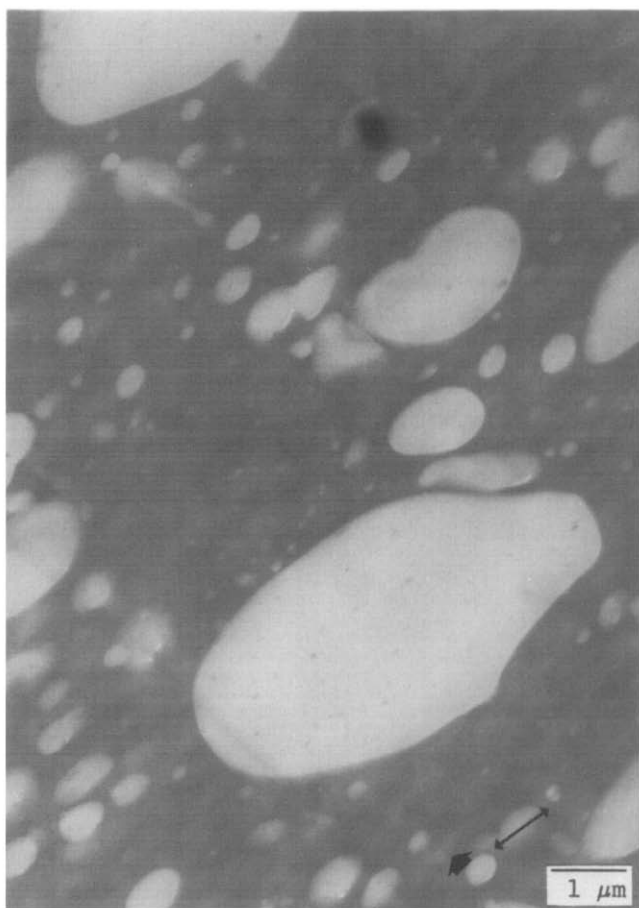


Figure 12 TEM micrograph of PSF/PPS blend (30/70 by weight) as moulded

The TEM micrographs may provide a possible explanation for the observed double glass transition temperatures. Figures 9a-c reveal that the dispersed domains are heterogeneous in size ranging from 35 nm to larger than

10 μm. The stratified sheets near the surface of the injection moulded specimen (Figure 9c) can be considered as large domain size. The stratified sheets near the surface are preserved by the rapid cooling of the melt near the mould surface. Those near the centre region of the specimen may break into small droplets upon cooling after injection moulding<sup>10</sup>. As the PPS content of the blends increases, the sheets become thicker and hence, even upon breakup, the resulting domains are large. Upon annealing, small domains may remain amorphous while larger domains are crystalline. The relationship of the droplet size and crystallizability can probably be explained in terms of a change from heterogeneous to homogeneous nucleation as the domain size decreases.

The formation of single-phase PPS droplets may be achieved through several avenues such as controlling the molecular weight, more extensive pre-blending (extrusion) and higher mould temperature to promote breakup of the stratified sheets after the mould is filled. Breakup of stratified sheets during flow leads to a compound morphology. Small droplets of PPS in the presence of PSF that remain in the amorphous state after annealing may be advantageous as far as mechanical properties are concerned.

## CONCLUSIONS

Melt mixing and subsequent injection moulding of polysulphone and poly(phenylene sulphide) form a phase separated material. With the described mixing and moulding conditions, at PPS concentrations < 10 wt%, the PPS does not crystallize upon annealing in the presence of PSF. At 20-35% PPS, two states of PPS are formed after annealing. A pure amorphous PPS state as well as a crystalline state is observed. However, above 35% PPS, the PPS phase tends to crystallize well due to the large size of the PPS domains. Both dynamic mechanical properties and the phase morphology allow

a consistent interpretation of the results. Small PPS domains remain amorphous; larger domains (including the stratified sheets) are crystalline. In addition, heat deflection temperatures of the blends at 1.8 MPa indicate that the deflection temperature is closely related to the continuous phase with slight influence from the dispersed domains.

The forming of small domain droplets may be achieved by carefully controlling the processing conditions such as shear rate, melt temperature, injection moulding pressure and mould surface temperature. Moreover, the molecular weight of the blend materials may be important too. A portion of PPS in the presence of PSF remains amorphous. This may be advantageous as crystalline PPS is rather brittle.

#### REFERENCES

- 1 Robeson, L. M. and Crisafulli, S. T. *J. Appl. Polym. Sci.* 1983, **28**, 2925
- 2 Brady, D. G. *J. Appl. Polym. Sci.* 1976, **20**, 2541
- 3 Zeng, H. and Mai, K. *Makromol. Chem.* 1986, **187**, 1787
- 4 Zeng, H., He, G. and Li, Y. *Polym. Commun.* (Institute of Polymer Science, Zhongshan University, Guangzhou) 1986, no. 2, 97
- 5 Zeng, H., He, G. and Yang, G. *Angew. Makromol. Chem.* 1986, **143**, 25
- 6 Nadkarni, V. M. and Jog, J. P. *J. Appl. Polym. Sci.* 1986, **32**, 5817
- 7 Swinyard, B. T., Barrie, J. A. and Walsh, D. J. *Polym. Commun.* 1987, **28**, 331
- 8 Cheng, S. Z. D., Wu, Z. Q. and Wunderlich, B. *Macromolecules* 1987, **20**, 2802
- 9 Struik, L. C. E. *Polymer* 1987, **28**, 1521, 1534
- 10 van Oene, H. J. *J. Coll. Interf. Sci.* 1972, **40**, 448